

Removal of Multiwalled Carbon Nanotube Contaminants from Surfaces with Microscale Topological Features

Zahra Karimi,^a Paul Su,^b Syed Hassan,^a Babak Haghpanah,^a William Doerr,^b and Ashkan Vaziri^a

^aDepartment of Mechanical and Industrial Engineering, Northeastern University, Boston, MA 02115; vaziri@coe.neu.edu (for correspondence)

^bFM Global, Norwood, MA 02062; pocheng.Su@fmglobal.com (for correspondence)

Published online 00 Month 2015 in Wiley Online Library (wileyonlinelibrary.com). DOI 10.1002/ep.12186

Experiments were performed to examine the efficiency of surfactants to remove multi-walled carbon nanotubes (MWCNTs) from silicon substrates with nano and micro-scaled features. In the first set of experiments, nanoscale features were induced on silicon wafers using SF₆ and O₂ plasma. In the second set, well-defined microscale topological features were induced on silicon wafers using photo lithography and plasma etching. The etching time was varied to create semi-ellipsoidal pits with average diameter and height of ~7–9 μm, and ~1–3 μm, respectively. For the cleaning process, the MWCNTs were wiped off using a simple wiping mechanism by two different surfactants and distilled water. The areal density of the MWCNTs was quantified prior to and after the removal using scanning electron microscopy (SEM) and post-image processing. For a surface featured with nanoscale asperities, the removal efficiency was measured to be in the range 83–99% based on substrate type and surface roughness. No evident relationship was observed between the etching time and the removal efficiency. For surfaces with microscale features, increasing the etching time results in appearance of larger pits and significant decrease in the removal efficiency. © 2015 American Institute of Chemical Engineers Environ Prog, 00: 000–000, 2015

Keywords: pollutant, nanomaterials

INTRODUCTION

Since their discovery in 1991, carbon nanotubes (CNTs) have attracted considerable attention due to their unique properties that include high stiffness, tensile strength, high Young's modulus, exceptional electrical conductivity, and excellent field emission [1–8]. The extremely small size and highly symmetrical structure of CNTs have allowed for remarkable quantum, magnetic, and electronic effects that are still being translated into exciting applications in the semiconductor industry [9–11]. However, health related concerns have been raised due to their high reactivity, large surface area and needle like structure [12, 13]. CNTs are considered to be carcinogenic and cause malignancy in the human mesothelial cells [14]. Their geometrical structure has been compared and shown to possess similar properties to asbestos fiber [12]. It is estimated that nanotechnology will

incorporate 15% of global manufacturing, totaling about \$2.6 trillion by 2014 [15]. CNTs can be used to develop novel biological and chemical sensors [16, 17]. For instance, carbon nanotube field-effect transistors can be used for detection of protein, antibody-antigen assays and DNA hybridization [16]. This ever increasing production of CNTs and potential health hazards due to their unwanted release into the work space have stimulated a demand for developing removal techniques for CNTs from contaminated surfaces. In case of an accidental spillage or release of CNTs, the main challenge in the removal process would be to overcome the adhesion, which is often treated as the molecular coupling between two contiguous bodies; here CNTs and the surface [18]. More specifically, as the particle size shrinks to microscale, the surface forces such as adhesion and friction become increasingly critical and dominate over inertial and gravitational forces [19]. Because of the high surface contact area of CNTs, their removal is difficult without application of an external force [20–22]. Several researchers have conducted adhesion related studies involving carbon nanotubes and different substrates [23–25]. The microwave treatment of Ni/Ti/Au/SiO₂/Si surfaces has proven to have enhanced their adhesion to carbon nanotubes [26]. Adhesion of MWCNTs to silicon oxide surfaces has been compared with the gecko's ability to climb vertically [24]. Whittaker *et al.* have calculated the vertical force of adhesion by using an Atomic Force Microscope (AFM) tip to slide a CNT into a carefully fabricated trench on a silicon dioxide substrate [23]. Buehler *et al.* showed that a long CNT can self-fold due to strong adhesion on the surface of a substrate [27].

The conventional approach for removal of residues from contaminated surfaces, generally known as solvent cleaning method, involves dispersion of contaminants in a cleaning medium and then removal of the cleaning medium with considerably less effort and higher efficiency due to the weaker bonds between solid and liquid phases. Two general approaches are used to disperse carbon nanotubes in various solvents: mechanical methods that involve either sonication (ultrasonic cleaning) or high shear mixing to mechanically disperse the CNTs [28], and physical or chemical methods that alter the surface energy of CNTs [29, 30]. In general, mechanical methods are not feasible for the purpose of decontamination since they have proven to be time-

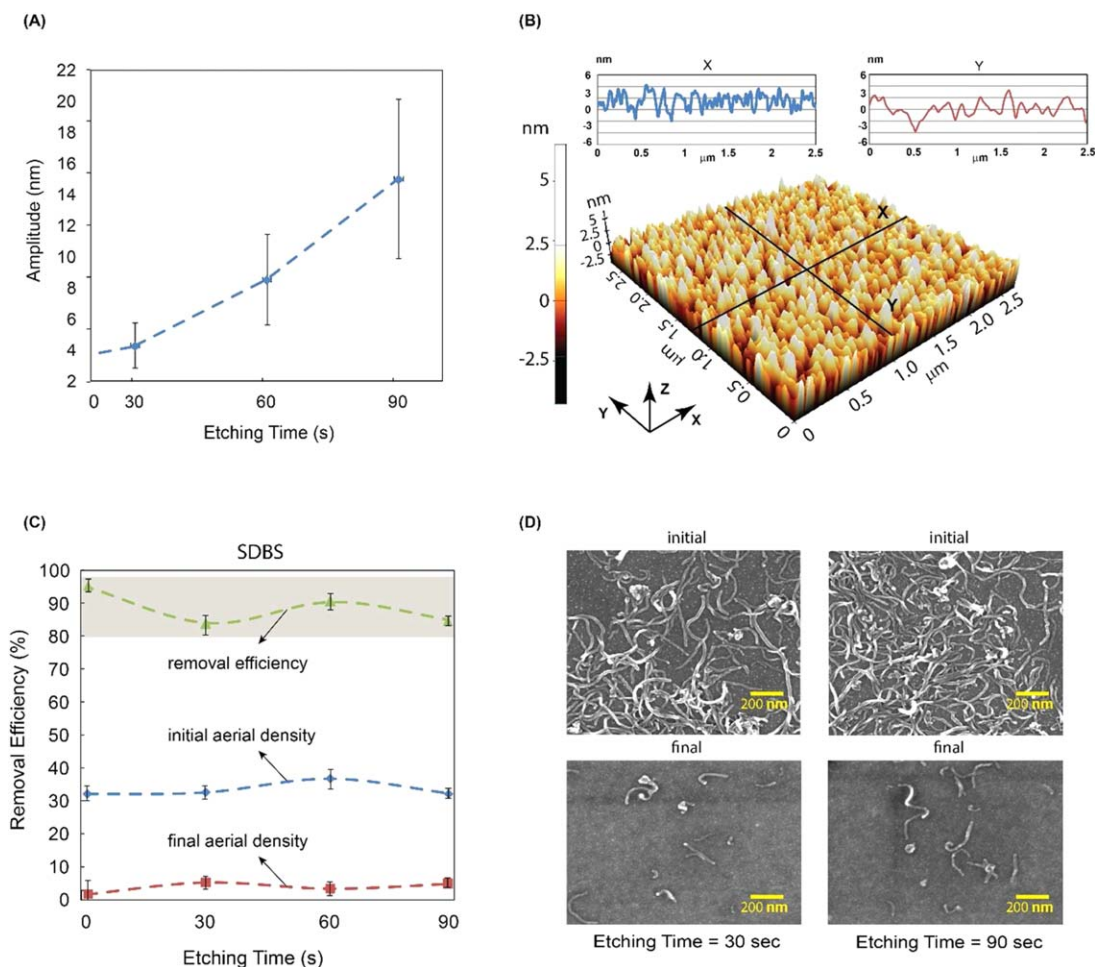


Figure 1. Surface analysis of silicon wafer after plasma etching for 30, 60, and 90 s. (A) Mean surface amplitude versus plasma etching time (s). Error bars indicate one standard deviation value; (B) AFM image of silicon substrate after surface was plasma (SF₆) etched for 30 s. (C) Plot of initial and final areal density and cleaning efficiency as a function of plasma (SF₆) etching time. (D) Sample SEM images of MWCNTs deposited on plasma treated silicon wafers after etching for 30 and 90 s before and after cleaning. [Color figure can be viewed in the online issue, which is available at [wileyonlinelibrary.com](http://www.wileyonlinelibrary.com).]

consuming and less efficient [28]. Furthermore, such energetic methods may lead to the wider spread of contamination [31, 32]. Chemical methods, also referred to as covalent treatment methods, involve using surface functionalization of carbon nanotubes at elevated temperatures and pressures to improve their solubility in solvent [33], making them unsuitable for *in situ* decontamination of the work space. Physical methods, which also are referred to as non-covalent treatment methods, use surfactants, solvents or polymers to disperse CNTs. These methods are widely used to disperse nanotubes since they absorb various groups of carbon nanotubes without altering the π -system of graphene [29, 30]. A variety of surfactants has been examined for this purpose such as octylphenol ethoxylate (Triton X-100) [34], dodecyltrimethylammonium bromide (DTAB) [35], sodium dodecylbenzenesulfonate (SDBS) [36] and sodium dodecylsulfate (SDS) [37]. These agents weaken the physical bond between surfaces and attached particles by reducing the surface tension and suppress particle re-adhesion by creating a repulsive zone by their amphiphilic (polar) mechanism [38]. It has been proposed that CNTs-surfactant complexes form spherical micelles in which CNTs form the core and surfactant molecules extend radially from the core [39–41]. Another morphology proposes that surfactant hemi-micellar aggregates cover carbon nanotubes [36, 42]. Angle of contact, chirality, diameter of CNTs

and concentration of SDS surfactant are important factors affecting CNT-surfactant adsorption [41, 43]. It is necessary that the amount of surfactant dissolved in the aqueous media should be far exceeding the surfactant critical micelle concentration to ensure that enough surfactant molecules can be absorbed onto the surface of the nanotubes to make them suspended and dissolved in water [44].

In our recent study [45], the removal of multi-walled carbon nanotubes (MWCNTs) from contaminated silicon wafers was carried out using sodium dodecylsulfate (SDS), sodium dodecylbenzenesulfonate (SDBS), Gum Arabic and calcium carbonate (CaCO₃). Silicon wafers were spin coated with MWCNTs. Scanning electron microscope (SEM) imaging and subsequent image processing were performed to estimate an average areal density prior and after cleaning. For cleaning, a fibrous material was soaked with each of the aforementioned chemicals and wiped across the surface manually. This study showed that surfactants can remove more than 95% of CNTs deposited on the smooth surface of a silicon wafer. In the current work, we present results of MWCNTs removal from rougher and corrugated surfaces of silicon by creating well-defined patterns using photo lithography and plasma treatment. The CNTs used for this study were combustion chemical vapor deposition (CCVD) grown, acid purified carbon nanotubes dispersed in polyvinylpyrrolidone (PVP) surfactant

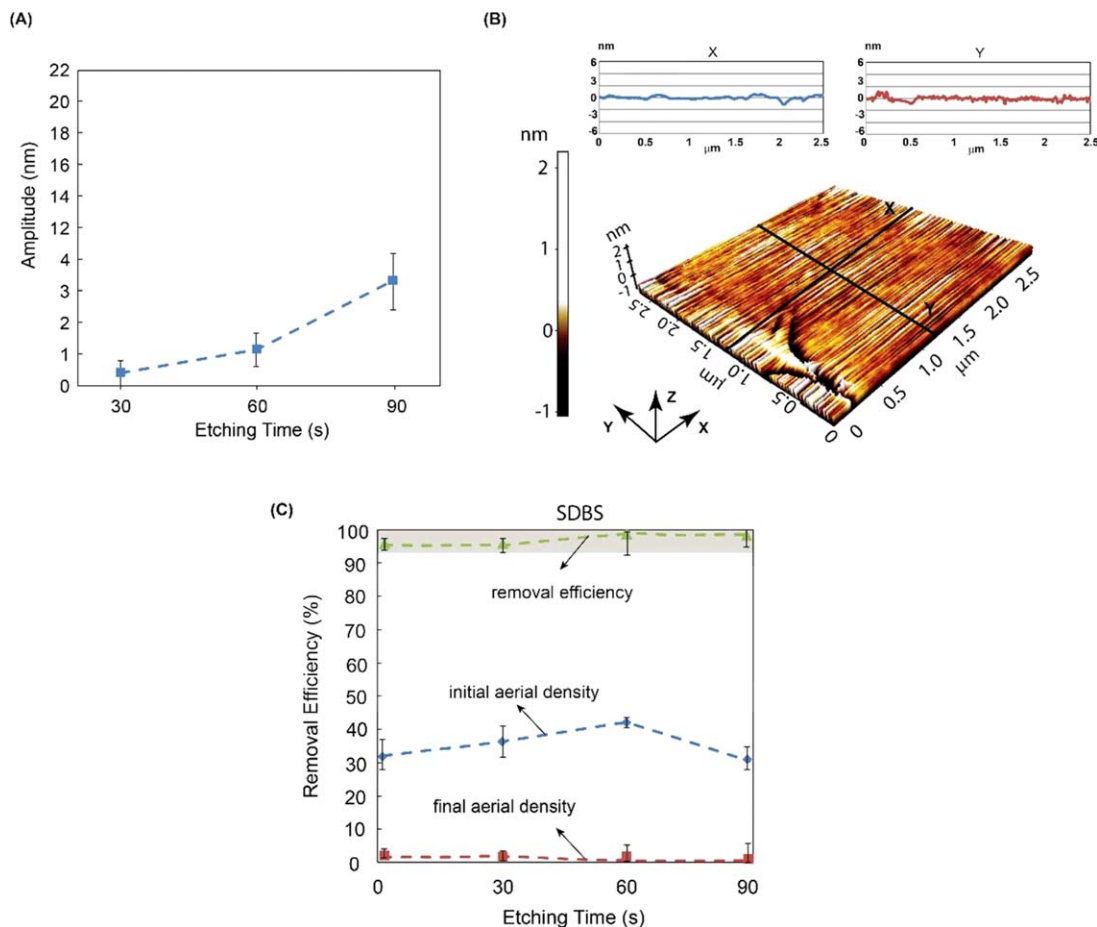


Figure 2. Surface analysis of silicon wafer after oxygen plasma treatment for 30, 60, and 90 s. (A) Mean surface amplitude versus plasma etching time (s). Error bars indicate one standard deviation value; (B) AFM image of silicon substrate after surface was oxygen plasma etched for 30 s. (C) Plot of initial and final areal density and cleaning efficiency as a function of plasma (O_2) treatment time. [Color figure can be viewed in the online issue, which is available at wileyonlinelibrary.com.]

which is commercially available. Wang *et al.* showed that homogenous and stable suspension of MWNTs aqueous can be produced by using polyvinylpyrrolidone [46]. The average length and diameter of the MWCNTs used in this study were measured to be 250 and 15 nm, respectively. In the current experimental study, the SDBS and SDS surfactant were chosen to disperse MWCNTs due to their demonstrated effectiveness and widespread application as CNT dispersants [47, 48].

METHODOLOGY AND EXPERIMENTS

Two different experimental methodologies were employed to create nano and microscale features on the surface of silicon wafers. In the first set of experiments, the surface of silicon wafers (Nitrogen/Phosphorus doped, P/E [polished and etched] surface, mechanical grade) were subjected to either of two different plasma treatments regimes, namely, SF_6 (20 sccm SF_6 , 10 sccm O_2 , 10 sccm Ar) and O_2 . The SF_6 plasma treatment was carried out in an Inductively Coupled Plasma (ICP) at 22°C, 10 mTorr, helium backside cooling. The experiments with O_2 treatment were performed in the Anatech SP-100 Plasma System. The plasma etching time was varied between 30 and 90 s, and the dependence of the amplitude of the created patterns on the etching time was quantified using non-contact high resolution atomic force microscope (AFM).

In the second set of experiments, microscale patterns were created on the surface of silicon wafers using a photolithography and plasma etching process. Positive photoresist

(Rohm Haas 1813) was spin-coated at 500 rpm for one minute. The wafer was then subjected to photolithography for ten seconds in a Quintel 4000 mask aligner to pattern mask features on the wafer surface. The wafer was later immersed in photoresist developer (MF-319 Rohm Haas) for 35–40 s. Plasma etching with SF_6 was performed on the wafer for 30 to 120 s (time range) in ICP plasma therm. Afterwards, the silicon wafers were immersed in a photoresist stripper solution (Shipley Microposit Remover1165) at 85°C for 5 min to remove the remaining photoresist polymer.

MWCNTs (dispersed in polyvinylpyrrolidone) were spin-coated on the etched wafers using a Laurell Spinner at 500 rpm for 60 s and then heated to 105°C for 90 s. Similar to our previous study [45]. SEM images were taken to estimate the initial areal density of MWCNTs on the substrate. For the removal process, three different cleaning media of SDS (4% technical grade in distilled water), SDBS (1.5% technical grade in distilled water), and pure distilled water were used. First, the cleaning medium was sprayed on the surface of the silicon wafer. After 2 min, the wafer was wiped once across the patterned surface using cleanroom wipes (non-woven polyester/cellulose), which were soaked in the cleaning medium (i.e., 100% saturation) for added efficiency. The wafer was manually wiped once. The estimated wiping pressure and duration were 2 kPa and 5 s. Thirty SEM images per wafer were taken after the cleaning, and image processing was performed in MATLAB [45] to measure the final areal density of MWCNTs.

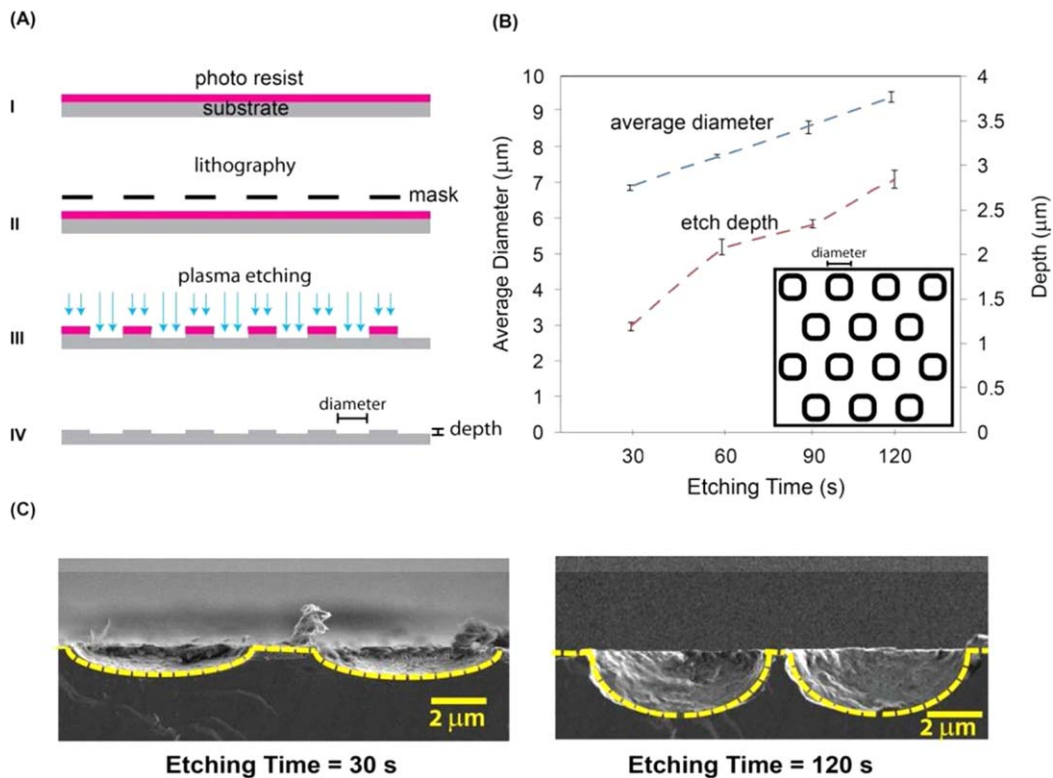


Figure 3. (A) Schematic of fabrication steps for creating surface topography on silicon wafers: (I) Spin coating positive photo-resist on silicon wafer; (II) Photolithography to pattern the mask; (III) Plasma etching; (IV) Stripping photo-resist. (B) Average diameter and pattern depth as a function of etching time. (C) SEM images of wafer side views, showing the surface features after etching for 30 and 120 s. [Color figure can be viewed in the online issue, which is available at wileyonlinelibrary.com.]

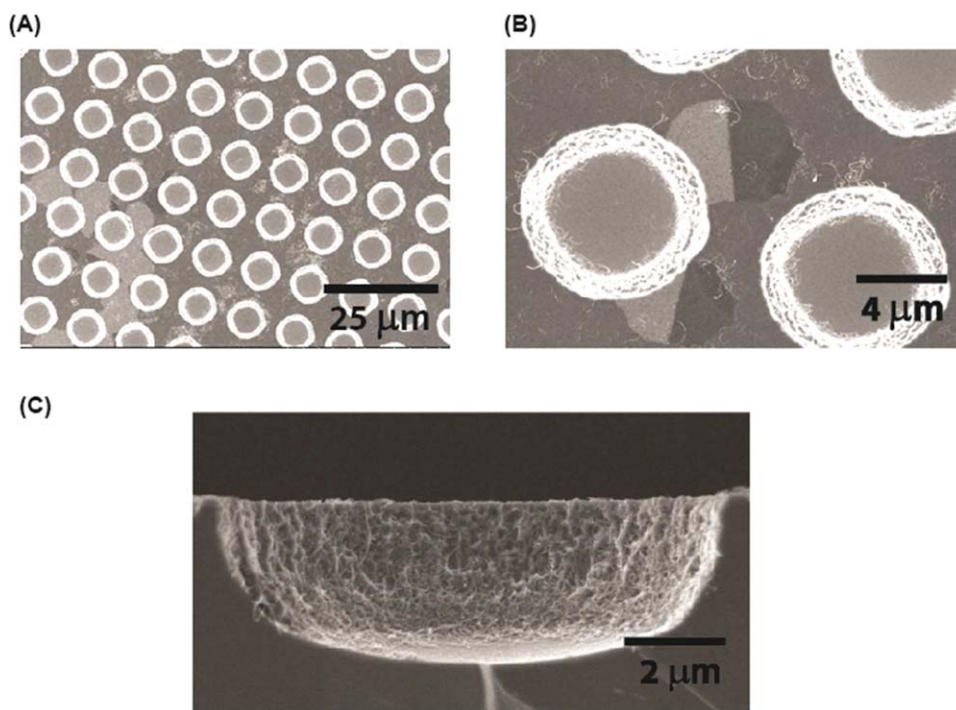


Figure 4. SEM images show distribution of MWCNTs around the walls of etched patterns. (A) and (B) show the wafers top view at different magnifications. (C) shows the side view of the wafers. The etching time was 120 s. [Color figure can be viewed in the online issue, which is available at wileyonlinelibrary.com.]

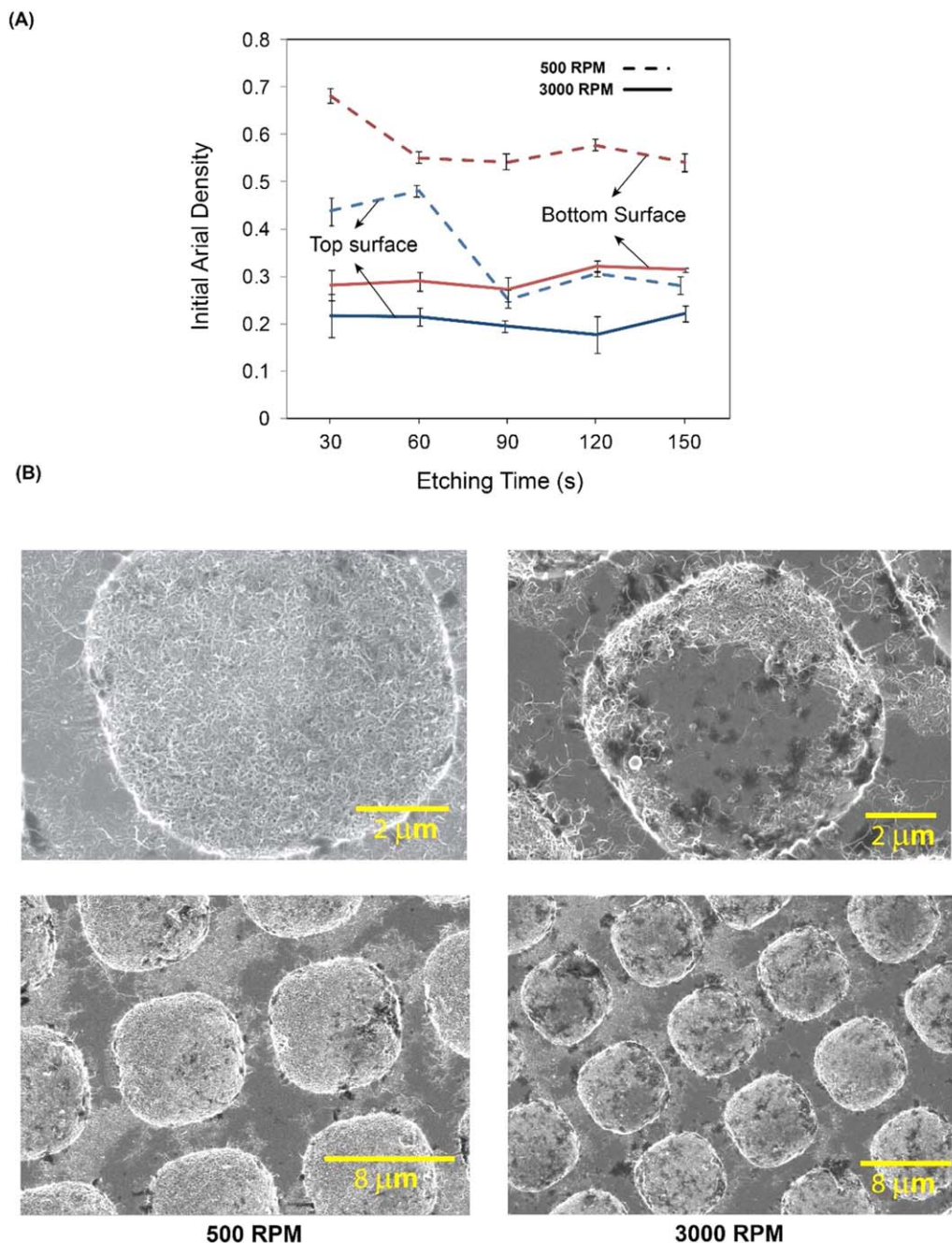


Figure 5. (A) Initial areal density distribution of MWCNTs at the top and bottom surfaces of the etched pattern after spin coating MWCNTs at different rpms, i.e., 500 and 3000; (B) SEM images of 30 s etched pattern shows the distribution of MWCNTs at 500 and 3000 rpm spinning at different magnifications. [Color figure can be viewed in the online issue, which is available at wileyonlinelibrary.com.]

The ability of different surfactants to remove CNTs from patterned surfaces was quantified by the removal efficiency parameter, defined as the difference between the initial and final areal density of MWCNTs divided by the initial areal density.

RESULTS AND DISCUSSION

Figure 1 shows a 3D image of a silicon surface of $2.7 \mu\text{m} \times 2.7 \mu\text{m}$ along with a graphical interpretation of the surface profile in the X and Y directions, respectively, after 30-s plasma treatment with SF₆. The amplitude presented in Figure 1A for the sample silicon substrate was measured by averaging the amplitude of the profile over an area of 5.72

μm^2 using XEI (Park Systems AFM software). The surface has nanoscale peaks and valleys with average amplitude of about 4 nm. Figure 2 shows the results for the O₂ plasma treatment. In general, treatment by the SF₆ plasma creates rougher features on the surface of the silicon wafer compared to the O₂ plasma treatment. Figures 1C and 2C show the efficiency of SDBS to remove MWCNTs from nano-patterned surfaces which were treated by the SF₆ and O₂ plasmas, respectively, versus the etching time. The efficiency of SDBS surfactant in removing MWCNTs for SF₆ plasma treated wafers is in the range of 83–93%, which is lower than the removal efficiency for the wafers treated with O₂ with efficiencies in the range of 95–99%. This can be attributed to

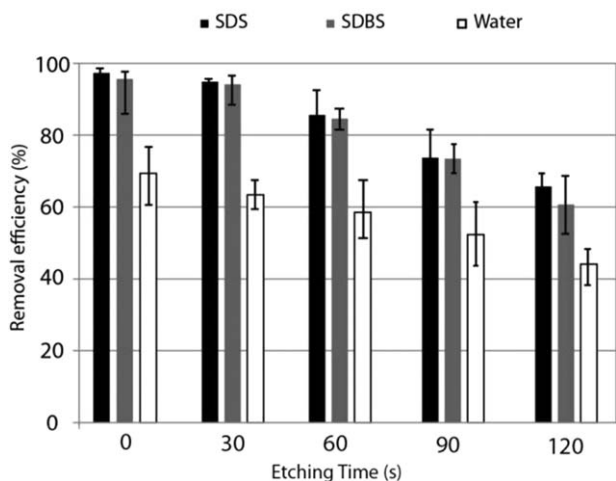


Figure 6. Removal efficiency of MWCNTs from top and bottom surfaces of Silicon wafers as a function of etching time; using water, SDS and SDBS.

higher roughness of the SF₆ plasma etched wafers, creating higher resistance to the removal process. SEM images of MWCNTs on silicon wafer treated with the SF₆ and O₂ plasma can be seen in Figure 1D before and after removal. As the roughness of the nanoscale featured surfaces increases, the removal efficiency of MWNTs from wafer surface is decreased. Also as the roughness increases, the contact area of wipe with surface decreases resulting in a decrease in the removal efficiency.

To study the effect of removal from the microscale mask patterns, as shown in Figure 3A photolithography and SF₆ plasma etching were used along with the micro fabrication. Figure 3B shows the dependence of the induced pattern diameter and etched depth on plasma treatment time. The inset shows the schematic of the mask patterns. The mask included 5 μm diameter circular holes separated by 5 μm space between adjacent patterns. Sample wafers with different etching times were cut in cross section and SEM imaging was performed to measure width and depth of etch as shown in Figure 3C. The average depth of the created patterns was varied between 1 and 3 μm for etching times of 30 and 120 s, respectively. The average pattern depth increases approximately linearly with increasing etching time. The average diameter of the created patterns increases slightly with increasing etching duration. The plasma etching process has some distinct advantages over other etching methods as it is easily repeatable, less sensitive to temperature changes and easier to start and shut down the procedure [49]. In the ICP plasma system a high density plasma discharge is generated by applying Radio Frequency (RF) power that is magnetically supplied through electromagnetic induction of an electric field. Figure 3C shows examples of the created patterns after plasma etching for 30 and 120 s.

The physiochemical properties of the surface can greatly influence the adhesion of carbon nanotubes to the substrate. This is particularly manifest in Figure 4, which illustrates the surface of a silicon wafer deposited with MWCNT after the etching process. The photoresist polymer still covers the non-etched portion of the wafer, whereas the rest of the photoresist free, imparting non-uniformity to the surface properties of silicon. As highlighted in Figures 4A and 4B, when MWCNTs were coated on the substrate their distribution was observed mostly in the proximity of circular pattern walls. Figure 4C shows a cross section of a pattern that indi-

cates strong adherence of nanotubes to the walls. To create a more uniform surface, a photoresist stripper was used to strip off the photoresist polymer from the “top” surface of the wafer. Also, plasma treatment was once again performed for 120 s to make sure that the whole surface is plasma etched and has uniform surface properties.

MWCNTs were spin coated on these surfaces at 500 and 3000 rpm. Figures 5A and 5B show comparison of spinning speed; the areal density of MWCNTs after spinning at 500 rpm is much greater than at 3000 rpm. Figure 5A is a graph of areal density distribution of MWCNTs in topological features created by plasma etching that indicates a higher number of nanotubes in the bottom surface (where were exposed to etching gases) as compared to the top surface (where were protected by photoresist from etching gases) of the etched pattern. This trend is most likely caused by the increased adhesion force of MWNTs to the substrate due to an increase in surface roughness, as evidenced by previous literature [50, 51].

For second set of experiment, the etching time was varied between 30 and 120 s and three samples were fabricated for each etching time step. The chart in Figure 6 shows a comparison of the removal efficiencies obtained by using two surfactants and water for different etching times from 0 to 120 s. The bars represent the removal efficiency averaged over the bottom and top surfaces which were created during the plasma etching. The removal efficiency on the top is constant for various etching times (and is represented by bars at etching time equal to 0) since the mask prevented any treatment on the top surfaces. As the result of plasma etching, the bottom surfaces were etched from 1 μm at the etching time of 30 s to 3 μm at the etching time of 120 s. As expected, increasing the etching time results in a decrease in the removal efficiency for all cleaning media due to increased surface roughness. There was no significant removal of MWCNTs inside the holes due to lack of contact between the wipe and contaminated surface, whereas the removal efficiency was much higher for the top surface because of sufficient removal force. This result highlights the important role of mechanical force in the decontamination process [52]. As the average depth of the micro scale features increases, the non-contact area of the wipe is expanded and the overall removal efficiency diminishes [52]. At equal depths of microscale features, SDS and SDBS both have greater removal efficiency than water. SDS shows slightly better decontamination efficiency compared to SDBS.

CONCLUSION

This research addresses the issue of MWCNTs removal from contaminated surfaces featured with controlled micro and nanoscale asperities. The average amplitude of the nanoscale asperities was varied between 1 and 15 nm by varying the etching time. The etching induced microscale semi-ellipsoidal pits had an average diameter and height of ~7–9 μm, and ~1–3 μm, respectively. The results show no evident correlation between the size of nanoscaled features and the removal efficiency. By varying the etching time, the removal efficiency is in the range of 83–93% and 95–99% for SF₆ and O₂ plasma etched surfaces, respectively. However, microscale morphological asperities on the substrate have the capacity to hold a great numbers of MWCNTs, which are difficult to remove by the wiping procedure. Increasing the size of these features significantly decreases the removal efficiency. Surfactants (SDS and SDBS) show a significant improvement in removal efficiency compared to water. The results of our study show that surfactant-saturated wipes can remove MWCNTs efficiently from contaminated surfaces; however their function is limited by the presence of microscale substrate roughness.

ACKNOWLEDGMENTS

The work was supported in part by the National Science Foundation CMMI Grant- 1149750, and in part by FM Global.

LITERATURE CITED

- Jorio, A., Dresselhaus, G., & Dresselhaus, M.S. (2008). Carbon nanotubes: Advanced topics in the synthesis, structure, properties and applications, New York: Springer Verlag.
- Das, M., Saxena, N., & Dwivedi, P.D. (2008). Emerging trends of nanoparticles application in food technology: Safety paradigms, *Nanotoxicology*, 3, 10–18.
- Balasubramanian, K. & Burghard, M. (2005). Chemically functionalized carbon nanotubes, *Small*, 1, 180–192.
- Dresselhaus, M., Dresselhaus, G., Eklund, P., & Saito, R. (2001). Carbon nanotubes: Synthesis, structures, and applications, Berlin: Springer.
- Ruoff, R.S., Qian, D., & Liu, W.K. (2003). Mechanical properties of carbon nanotubes: Theoretical predictions and experimental measurements, *Comptes Rendus Physique*, 4, 993–1008.
- Salvetat, J.P., Bonard, J.M., Thomson, N., Kulik, A., Forro, L., Benoit, W., & Zuppiroli, L. (1999). Mechanical properties of carbon nanotubes, *Applied Physics A: Materials Science & Processing*, 69, 255–260.
- Hsu, C.H., Chen, C.F., Chen, C.C., & Chan, S.Y. (2005). Density-controlled carbon nanotubes, *Diamond and Related Materials*, 14, 739–743.
- Ebbesen, T., Lezec, H., Hiura, H., Bennett, J., Ghaemi, H., & Thio, T. (1996). Electrical conductivity of individual carbon nanotubes, *Nature*, 382, 54–56.
- Schelling, P. K., Phillpot, S. R., & Keblinski, P. (2002). Comparison of atomic-level simulation methods for computing thermal conductivity. *Physical Review B*, 65(14), 144306.
- Yakobson, B.I., Brabec, C., & Bernholc, J. (1996). Nanomechanics of carbon tubes: Instabilities beyond linear response, *Physical Review Letters*, 76, 2511–2514.
- Meyyappan, M. (2005). Carbon nanotubes: Science and applications, Boca Raton, FL: CRC.
- McCarthy, N. (2012). Nanotechnology: Size matters. *Nature Reviews Cancer*, 12, 7–7.
- Dowling, A. (2004). Nanoscience and nanotechnologies: Opportunities and uncertainties, London: Royal Society and Royal Academy of Engineering.
- Nagai, H., Okazaki, Y., Chew, S.H., Misawa, N., Yamashita, Y., Akatsuka, S., Ishihara, T., Yamashita, K., Yoshikawa, Y., & Yasui, H. Diameter and rigidity of multi-walled carbon nanotubes are critical factors in mesothelial injury and carcinogenesis, *Proceedings of the National Academy of Sciences USA*, 108, E1330–E1338.
- Bowman, D.M. & Hodge, G.A. Nanotechnology and public interest dialogue: Some international observations, *Bulletin of Science, Technology & Society*, 27, 118–132.
- Allen, B.L., Kichambare, P.D., & Star, A. (2007). Carbon nanotube field-effect-transistor-based biosensors, *Advanced Materials*, 19, 1439–1451.
- Ellis, J.E., Green, U., Sorescu, D.C., Zhao, Y., & Star, A. (2015) Indium oxide—single-walled carbon nanotube composite for ethanol sensing at room temperature, *The Journal of Physical Chemistry Letters*, 6, 712–717.
- Entsiklopediya, S.I. (1961). Soviet historical encyclopedia, Moscow Izdat. Soviet Ents, 7.
- Bhushan, B. (1998). Tribology issues and opportunities in MEMS: Proceedings of the NSF/AFOSR/ASME Workshop on Tribology Issues and Opportunities in MEMS held in Columbus, Ohio, USA, 9-11 November 1997, Springer.
- Krishnan, S., Busnaina, A., Rimai, D., DeMejo, L. The adhesion-induced deformation and the removal of submicrometer particles, *Journal of Adhesion Science and Technology*, 8, 1357–1370.
- Gale, G. & Busnaina, A. (1995). Removal of particulate contaminants using ultrasonics and megasonics: A review, *Particulate Science and Technology*, 13, 197–211.
- Karimi, P., Ahmed, A.B., Bong, K.K. & Jin, G.P. (2013). Non destructive nanoparticle removal from sub-micron structures using megasonic cleaning, *Solid State Phenomena*, 195, 191–194.
- Whittaker, J.D., Minot, E.D., Tanenbaum, D.M., McEuen, P.L., & Davis, R.C. (2006). Measurement of the adhesion force between carbon nanotubes and a silicon dioxide substrate, *Nano Letters*, 6, 953–957.
- Qu, L., Dai, L., Stone, M., Xia, Z., & Wang, Z.L. (2008). Carbon nanotube arrays with strong shear binding-on and easy normal lifting-off, *Science*, 322, 238–242.
- Zhou, W., Huang, Y., Liu, B., Wu, J., Hwang, K., & Wei, B. (2007). Adhesion between carbon nanotubes and substrate: Mimicking the Gecko foot-hair, *Nano*, 2, 175.
- Su, H.C., Chen, C.H., Chen, Y.C., Yao, D.J., Chen, H., Chang, Y.C., & Yew, T.R. (2010). Improving the adhesion of carbon nanotubes to a substrate using microwave treatment, *Carbon*, 48, 805–812.
- Buehler, M.J., Kong, Y., Gao, H., & Huang, Y. (2006). Self-folding and unfolding of carbon nanotubes, *Journal of Engineering Materials and Technology*, 128, 3.
- Lu, K., Lago, R., Chen, Y., Green, M., Harris, P., & Tsang, S. (1996). Mechanical damage of carbon nanotubes by ultrasound, *Carbon*, 34, 814–816.
- Rastogi, R., Kaushal, R., Tripathi, S., Sharma, A.L., Kaur, I., & Bharadwaj, L.M. (2008). Comparative study of carbon nanotube dispersion using surfactants, *Journal of Colloid and Interface Science*, 328, 421–428.
- Vaisman, L., Wagner, H.D., & Marom, G. (2006). The role of surfactants in dispersion of carbon nanotubes, *Advances in Colloid and Interface Science*, 128, 37–46.
- Heinemann, M. & Schäfer, H.G. (2009). Guidance for the handling and use of nanomaterials at the workplace. *Human & experimental toxicology*, 28.6-7, 407–411.
- British Standard Institute. (2007). Nanotechnologies—Part 1: Good practices guide for specifying manufactured nanomaterials. Available at: <http://www3.imperial.ac.uk/pls/portallive/docs/1/34683697.PDF>.
- Hilding, J., Grulke, E.A., George Zhang, Z., & Lockwood, F. (2003). Dispersion of carbon nanotubes in liquids, *Journal of Dispersion Science and Technology*, 24, 1–41.
- Wang, H., Zhou, W., Ho, D.L., Winey, K.I., Fischer, J.E., Glinka, C.J., & Hobbie, E.K. (2004). Dispersing single-walled carbon nanotubes with surfactants: A small angle neutron scattering study, *Nano Letters*, 4, 1789–1793.
- Whitsitt, E.A. & Barron, A.R. (2003). Silica coated single walled carbon nanotubes, *Nano Letters*, 3, 775–778.
- Islam, M., Rojas, E., Bergey, D., Johnson, A., & Yodh, A. (2003). High weight fraction surfactant solubilization of single-wall carbon nanotubes in water, *Nano Letters*, 3, 269–273.
- Yu, J., Grossiord, N., Koning, C.E., & Loos, J. (2007). Controlling the dispersion of multi-wall carbon nanotubes in aqueous surfactant solution, *Carbon*, 45, 618–623.
- Ng, D., Huang, P., Jeng, Y., & Liang, H. (2007). Nanoparticle removal mechanisms during post-CMP cleaning, *Electrochemical and Solid-State Letters*, 10, H227.
- Hagen, A. & Hertel, T. (2003). Quantitative analysis of optical spectra from individual single-wall carbon nanotubes, *Nano Letters*, 3, 383–388.
- O'Connell, M.J., Boul, P., Ericson, L.M., Huffman, C., Wang, Y., Haroz, E., Kuper, C., Tour, J., Ausman, K.D., & Smalley, R.E. (2001). Reversible water-solubilization of

- single-walled carbon nanotubes by polymer wrapping, *Chemical Physics Letters*, 342, 265–271.
41. Wallace, E.J. & Sansom, M.S.P. (2007). Carbon nanotube/detergent interactions via coarse-grained molecular dynamics, *Nano Letters*, 7, 1923–1928.
 42. Poulin, P., Vigolo, B., & Launois, P. (2002). Films and fibers of oriented single wall nanotubes, *Carbon*, 40, 1741–1749.
 43. Tummala, N.R. & Striolo, A. (2009). SDS surfactants on carbon nanotubes: Aggregate morphology, *ACS Nano*, 3, 595–602.
 44. Sun, Z., Nicolosi, V., Rickard, D., Bergin, S.D., Aherne, D., & Coleman, J.N. (2008). Quantitative evaluation of surfactant-stabilized single-walled carbon nanotubes: Dispersion quality and its correlation with zeta potential, *The Journal of Physical Chemistry C*, 112, 10692–10699.
 45. Su, P., Haghpanah, B., Doerr, W. W., Karimi, Z., Hassan, S., Gritzo, L., Busnaina, A.A., & Vaziri, A. (2014). Decontamination of surfaces exposed to carbon-based nanotubes and nanomaterials, *Journal of Nanomaterials*, 2014.
 46. Wang, B., Liu, S., Zhu, Y., & Ge, S. (2014). Influence of polyvinyl pyrrolidone on the dispersion of multi-walled carbon nanotubes in aqueous solution, *Russian Journal of Physical Chemistry A*, 88, 2385–2390.
 47. Jiang, L., Gao, L., & Sun, J. (2003). Production of aqueous colloidal dispersions of carbon nanotubes, *Journal of Colloid and Interface Science*, 260, 89–94.
 48. Wang, J., Sun, J., Gao, L., Liu, Y., Wang, Y., Zhang, J., Kajiura, H., Li, Y.M., and Noda, K. (2009). Improving the conductivity of single-walled carbon nanotubes films by heat treatment, *Journal of Alloys and Compounds*, 485, 456–461.
 49. Campbell, S.A. (2001). *Science and engineering of micro-electronic fabrications*, USA: Oxford.
 50. Wong, H.-C., Umehara N., & Kato, K. (1998). The effect of surface roughness on friction of ceramics sliding in water, *Wear*, 218, 237–243.
 51. Li, J., Xia, L., Li, P., Zhu, Y., Sun, Y., & Zuo, D. (2013). Relationship between coefficient of friction and surface roughness of wafer in nanomachining process," in *Fourth International Conference on Smart Materials and Nanotechnology in Engineering*, Ed., pp. 87931Y-87931Y-87936, International Society for Optics and Photonics, 2013.
 52. Patrick, W.J., Guthrie, W.L., Standley, C.L., & Schiabe, P.M. (1991) Application of chemical mechanical polishing to the fabrication of VLSI circuit interconnections, *Journal of the Electrochemical Society*, 138, 1778–1784.
-